IEEE Access
Multidisciplinary | Rapid Review | Open Access Journal

Received 22 August 2022, accepted 9 September 2022, date of publication 14 September 2022, date of current version 21 September 2022.

Digital Object Identifier 10.1109/ACCESS.2022.3206548

RESEARCH ARTICLE

Feasibility of a Plasma-Based Intelligent Reflective Surface

MIRKO MAGAROTTO[1], LUCA SCHENATO[2,3], (Member, IEEE), PAOLA DE CARLO[4], AND ANTONIO-DANIELE CAPOBIANCO[3,5], (Member, IEEE)

[1]Department of Industrial Engineering, University of Padova, 35131 Padova, Italy
[2]National Research Council, 35127 Padova, Italy
[3]National Inter-University Consortium for Telecommunications, CNIT, 43124 Parma, Italy
[4]Technology for Propulsion and Innovation S.P.A., 35121 Padova, Italy
[5]Department of Information Engineering, University of Padova, 35131 Padova, Italy

Corresponding author: Mirko Magarotto (mirko.magarotto@unipd.it)

ABSTRACT Gaseous Plasma Antennas are devices in which an ionized gas (i.e., plasma) is exploited to transmit and receive Electromagnetic waves. Their main advantage over metallic systems is the possibility to reconfigure the antenna performance (e.g., radiation pattern) by electronically varying the plasma parameters (e.g., density). Recently, Intelligent Reflecting Surfaces (IRSs) have been proposed to control the environment between transmitting and receiving antennas manipulating the signals reflected. In this work, the feasibility of a plasma-based IRS is investigated. A theoretical model has been developed to assess the use of plasma as a reflecting medium. Numerical simulations have been performed to preliminary design plasma-based IRSs. Two designs of IRSs, relying on plasma properties consistent with the technology at the state-of-the-art, are proposed. The former enables beam steering operations depending on the continuous control of the phase of the reflected wave. The latter exploits a 1-Bit coding strategy to produce specific diffraction patterns. The main advantage of a plasma-based IRS with respect to the metallic counterpart is the possibility to control the phase of the reflected wave, maintaining the magnitude of the reflection coefficient close to the unit. The main drawback of plasma-based systems is the necessity of using thick plasma elements (in the order of the wavelength in the air) to control the phase of the reflected wave over 360 deg. This constraint can be relaxed if digital plasma elements are adopted.

INDEX TERMS Gaseous plasma antennas, intelligent reflective surfaces, reconfigurable antennas.

I. INTRODUCTION

In recent years, there has been a growing interest in a new class of antennas that exploit an ionized gas, namely plasma, to transmit and receive Electromagnetic (EM) waves. These devices are called Gaseous Plasma Antennas (GPAs) [1]. GPAs present several advantages with respect to conventional metallic antennas, providing the possibility to control the EM response of the plasma electronically [2]. First, the plasma is produced by energizing a neutral gas confined inside a dedicated vessel. Namely, when a GPA is off, it is characterized by a reduced Radar Cross Section (RCS) given the absence of the main conductive medium (i.e., plasma) [3]. This feature reduces the mutual interference between antennas stacked into arrays [4]. Moreover, the capability to electrically "disappear" is very appealing if stealth is required [5]. Second, the figures of merit of a GPA (e.g., operation frequency and radiation pattern) can be reconfigured by controlling the electric power used to sustain the plasma. The latter determines the plasma density and temperature, which, in turn, drives the EM response [6]. Third, plasma is a dispersive medium; namely, co-site interference levels can be minimized for GPAs operated at different frequencies [7].

Several architectures have been proposed to exploit the capabilities of GPAs. Borg *et al.* [8] realized a monopole antenna operated in the 3–150 MHz frequency range relying on a surface wave-driven discharge. Anderson *et al.* [1] proposed a GPA working in the 0.5–20 GHz frequency range in which the plasma is sustained in DC or pulsed-DC mode. De Carlo *et al.* [9] realized a plasma dipole

The associate editor coordinating the review of this manuscript and approving it for publication was Pavlos I. Lazaridis.

operated in the Ultra High Frequency (UHF) range relying on custom-build Cold Cathodel Fluorescence Lamps (CCFL). Numerical designs of both transmit-arrays [10], [11], Yagi-Uda antennas [12], and plasma panels [13] envisioned the use of passive plasma discharges as signal directors. Passive plasma discharges are also employed to realize reflect-arrays. Melazzi *et al.* [14] built a reflect-array for satellite-based radio navigation (i.e., Galileo frequency range 1.164–1.592 GHz). The prototype comprises a metallic dipole surrounded by a set of CCFLs capable of beam-forming operations by electronically switching on and off the plasma discharges. Similarly, CCFLs have been used by Jusoh *et al.* [15] to realize a corner reflector antenna fed by a monopole device operated at 2.4 GHz, with a maximum gain 10.8 dBi and based on a similar beam-forming mechanism. Zainud-Deen *et al.* [16] proposed a numerical design of a reflect-array in which plasma cells can be used to control the phase of the reflected wave. In this way, the authors achieved beam steering operations by tuning the plasma properties of each cell, namely adjusting the electrical feeding power.

The advent of commercial 5G and the forthcoming next-generation communications have boosted academia [17] and industry's interest [18] in developing novel technologies to accommodate different communication protocols and handle adverse channel conditions. Among these technologies, Intelligent Reflecting Surfaces (IRSs), also known as Reconfigurable Intelligent Surfaces, are engineered, programmable planar structures capable of controlling the scattering and reflection of radio signals by tuning the EM properties of the surface [19], [20], [21], either implemented by phased arrays or metasurfaces [22]. Specifically, a metasurface is a planar array consisting of a large number of digitally controllable elements called meta-atoms [23], [24]. IRSs change the paradigm that the medium between the transmitter and the receiver antennas is a random entity. Indeed, introducing an IRS into the environment makes it possible to control the phase, amplitude, polarization, and even the frequency of the reflected signals [25]. Thus the propagation environment is upgraded into an entity that can be programmed and optimized, i.e., the smart radio environment [26], [27]. The key feature of IRSs, namely the passive and tunable reflected signal transformation, is usually achieved by integrating active elements (e.g., PIN or varactor diodes) in the unit cells that constitute the surfaces. Each unit cell can independently change the amplitude and phase of the impinging signal to produce a reflecting fine beam shaping synergically. Additionally, IRSs allow the reuse of ambient signals for communications instead of creating new ones, enabling low-power communications and reducing EM pollution. In this sense, IRSs break new ground to mitigate the detrimental effect of the surrounding medium and respond to the need for higher data rates and energy efficiency in 5G and emerging 6G technologies.

The present study explores the feasibility of plasma-based IRSs. This concept is worth investigating, provided the plasma's capability to act as a reflector and the possibility to control the phase of the reflected wave by varying the plasma density electronically [16]. Using a plasma panel to accomplish beam steering operations is not new [16]. Nonetheless, this study introduces relevant advances to the state-of-the-art. First and differently from previous works [16], the proposed design relies on realistic plasma properties. The assumed values of plasma density, electron temperature, and neutral gas pressure are coherent with the experimental data available in the literature of GPAs [4]. Specifically, for each configuration proposed dedicated experimental works have been referenced to demonstrate the feasibility of the design. Therefore, the results discussed in the following are more robust with respect to previous works in which aspirational plasma properties have been assumed [28] (e.g., inconsistent plasma density and neutral pressure). Second, we derive quantitative design rules valid for a generic plasma panel operated as a reflector. This result improves the state-of-the-art since past configurations address only peculiar architectures (e.g., the incident wave produced by a horn antenna [16]). Specifically, a simplified theoretical model has been developed to assess the use of plasma as a reflecting medium.

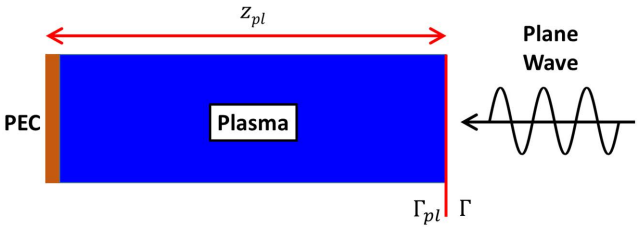

FIGURE 1. Schematic of the plasma element analysed with the theoretical model.

Eventually, the remainder part of this paper is organized as follows. Section II discusses the adopted theoretical-numerical methodology. Section III and Section IV present the derivation of the quantitative design rules and the numerical design of two plasma-based IRSs, respectively. Finally, Section V draws the conclusions and discusses the next steps toward realizing a plasma-based IRS.

II. METHODOLOGY

A theoretical model has been developed to assess the use of plasma as a reflecting medium, and numerical simulations are performed to preliminary design plasma-based IRSs. In both cases, the EM response of the plasma, namely its capability to control the phase of the reflected wave, is described via the relative permittivity ε_r. The latter is derived according to the cold plasma model [29]. The motion of the ions has been neglected provided the frequencies of interest are in the GHz range [29]. Namely, ε_r reads:

$$\varepsilon_r = 1 - \frac{\omega_p^2}{\omega^2 + \nu^2} + j\frac{\nu}{\omega}\frac{\omega_p^2}{\omega^2 + \nu^2} \tag{1}$$

where ω is the wave angular frequency in rad/s, ω_p is the plasma frequency in rad/s, ν is the collision frequency in Hz, and j is the imaginary unit. The plasma frequency is given

by [29]

$$\omega_p = \sqrt{\frac{q^2 n_e}{m\varepsilon_0}} \tag{2}$$

where q is the elementary charge, m is the electron mass, ε_0 is the vacuum permittivity, and n_e is the plasma density in m^{-3}. Specifically, n_e and, in turn, ω_p depend on the electric power to sustain the plasma [6], namely they are the parameters used to control electronically ε_r and the phase of the reflected wave. The collision frequency is determined by the electron-neutral elastic scattering reaction, which is the most relevant dissipation mechanism for usual GPAs [4], [30]. Its expression follows [31]

$$\nu = n_0 K(T_e) \tag{3}$$

where n_0 is the density of neutral particles in m^{-3}, and K is a rate constant that depends on the electron temperature T_e, as [31]:

$$K = 2.336 \times 10^{-14} T_e^{1.609} \times \exp\left(0.0618(\ln T_e)^2 - 0.1171(\ln T_e)^3\right) \tag{4}$$

where T_e is expressed in eV. It is worth defining three additional parameters to provide a complete description of the plasma. First, the neutral pressure p_0, whose expression reads [31]:

$$p_0 = k_B T_0 n_0 \tag{5}$$

where k_B is the Boltzmann constant, and T_0 is the neutral gas temperature in K. Second, the plasma impedance

$$Z_{pl} = \frac{Z_0}{\sqrt{\varepsilon_r}} \tag{6}$$

where $Z_0 = \sqrt{\mu_0/\varepsilon_0}$ is the impedance of free space, and μ_0 is the vacuum permeability. Third, the critical density n_e^{cr}, which reads [31]:

$$n_e^{cr} = m\varepsilon_0 \left(\frac{2\pi f}{q}\right)^2 \tag{7}$$

where $f = \omega/2\pi$ is the wave frequency in Hz. The parameter n_e^{cr} indicates the plasma density for which $\omega = \omega_p$. For $n_e \lesssim n_e^{cr}$ waves can propagate in plasma since $\mathrm{Re}(\varepsilon_r) > 0$. For $n_e \gtrsim n_e^{cr}$ only evanescent waves occur within plasma being $\mathrm{Re}(\varepsilon_r) < 0$ [29]. From now on, the condition $n_e \lesssim n_e^{cr}$ is referred to as the dielectric regime and $n_e \gtrsim n_e^{cr}$ as the conductor regime. Equivalently, the dielectric regime occurs for $f \gtrsim \omega_p/2\pi$, and the conductor ones for $f \lesssim \omega_p/2\pi$.

A. THEORETICAL MODEL

A simplified theoretical model has been developed to assess the use of plasma as a reflector. A schematic of the considered setup is depicted in Fig. 1. A homogeneous plasma slab of thickness z_{pl}, located on top of an infinite Perfect Electric Conductor (PEC) constituting the ground plane [16], is orthogonally impinged by a linearly polarized plane wave.

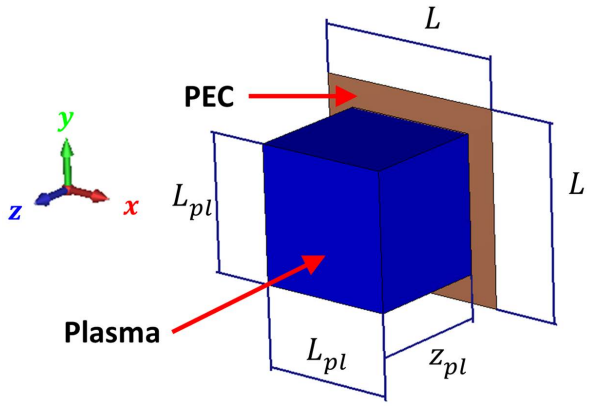

FIGURE 2. Schematic of the plasma element analysed with the numerical model.

The reflected wave is described via the complex reflection coefficient Γ defined as

$$\Gamma = \frac{E_\rho}{E_\iota} \tag{8}$$

where E_ρ and E_ι are the reflected and incident electric field, respectively. According to the conventional transmission line model [32], Γ reads

$$\Gamma = \frac{\rho + \Gamma_{pl}}{1 + \rho\Gamma_{pl}} \tag{9}$$

where ρ is the Fresnel's reflection coefficient at the air-plasma interface, and Γ_{pl} is the reflection coefficient within the plasma medium. Specifically, Γ_{pl} reads

$$\Gamma_{pl} = -\exp\left(j\,4\pi\sqrt{\varepsilon_r}\frac{z_{pl}}{\lambda}\right) \tag{10}$$

where $\lambda = c/f$ is the wavelength in air, and ρ reads

$$\rho = \frac{Z_{pl} - Z_0}{Z_{pl} + Z_0} = \frac{1 - \sqrt{\varepsilon_r}}{1 + \sqrt{\varepsilon_r}} \tag{11}$$

B. NUMERICAL MODEL

Numerical analyses have been accomplished with the commercial software CST microwave Studio®. The schematic of a plasma element is reported in Fig. 2. A plasma element of thickness z_{pl} and width L_{pl} is placed on top of a PEC ground plane whose side has dimension L, which represents the lattice periodicity. The computational domain has been discretized on an unstructured tetrahedral mesh and Maxwell's equations integrated in the frequency domain. An incident plane wave propagating along the z direction is assumed to impact normally the plasma elements. Two types of simulations have been performed: (i) single element analysis to compute the reflection coefficient Γ, and (ii) array analysis to evaluate the radiation pattern scattered by the plasma panel. The single element analysis is accomplished assuming Floquet boundary conditions along the x and y directions; an open condition is assumed along z [33]. Instead, open boundary conditions have been adopted to compute the RCS of the IRS.

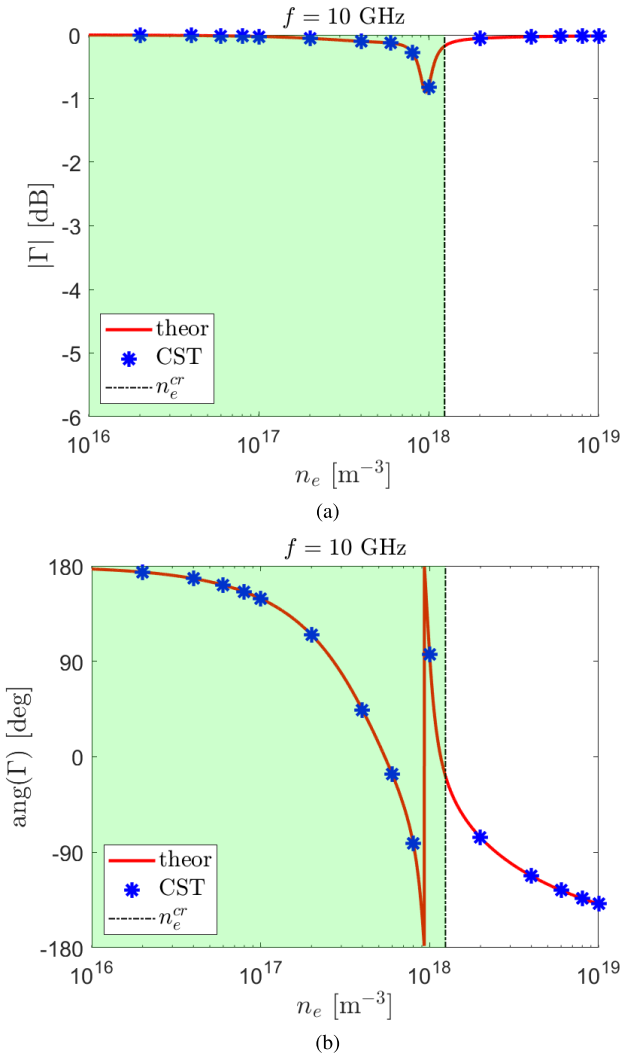

FIGURE 3. (a) Magnitude, and (b) phase of the reflection coefficient Γ in function of the plasma density n_e. Comparison between theoretical (theor) and numerical (CST) models. $z_{pl} = \lambda$, $n_0 = 10^{22}$ m^{-3} ($p_0 = 0.4$ mbar), and $\nu = 3.1 \times 10^8$ Hz. Green background indicates the dielectric regime, white background the conductor regime.

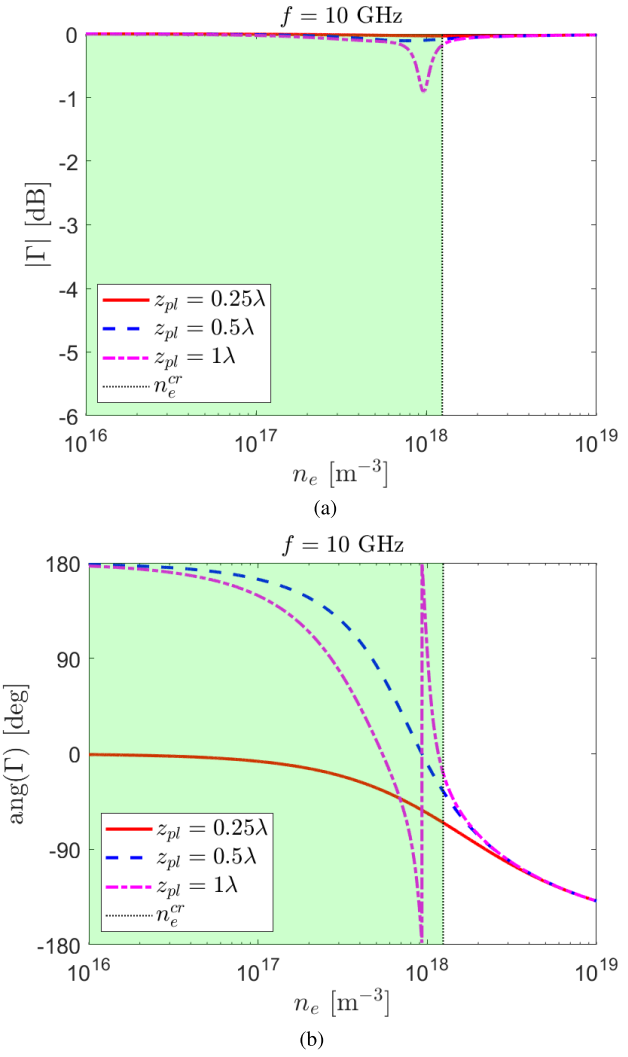

FIGURE 4. (a) Magnitude, and (b) phase of the reflection coefficient Γ in function of the plasma density n_e. Comparison between different values of the plasma thickness z_{pl}. $n_0 = 10^{22}$ m^{-3} ($p_0 = 0.4$ mbar), and $\nu = 3.1 \times 10^8$ Hz. Green background indicates the dielectric regime, white background the conductor regime.

III. THEORETICAL ANALYSIS

The theoretical model has been: (i) verified against numerical results and (ii) exploited to derive quantitative design rules for the plasma element.

A. VERIFICATION

To verify the reliability of the theoretical model, its results have been compared against a numerical benchmark. The working frequency is assumed equal to $f = 10$ GHz [34], the thickness of the plasma slab is $z_{pl} = \lambda = 30$ mm. The values selected for the plasma parameters are consistent with measures performed on actual GPA prototypes [4], [35]. The neutral density is equal to $n_0 = 10^{22}$ m^{-3}, namely $p_0 = 0.4$ mbar [35]. The electron temperature is equal to $T_e = 1.2$ eV [4], namely $\nu = 3.1 \times 10^8$ Hz. The plasma density (i.e., the parameter that allows to tune the wave reflection electronically) is varied from 10^{16} m^{-3} up to 10^{19} m^{-3} [5], thus theoretical and numerical results are cross-checked in a broad operative range. Consistently, ω_p varies from 5.6×10^9 rad/s up to 1.8×10^{11} rad/s. Numerical simulations of a single plasma element are performed assuming $L_{pl} = L$, following the theoretical model assumptions. Provided the imposed Floquet boundary conditions, the numerical results are not dependent on the value of L nonetheless the assumption $L = \lambda/2 = 15$ mm has been made. An excellent agreement between theoretical and numerical results is obtained (see Fig. 3): differences are lower than 1% in terms of both the amplitude and phase of Γ.

B. PLASMA ELEMENT ANALYSIS

The theoretical model has been exploited to evaluate the sensitivity of Γ to n_e and z_{pl} (see Fig. 4). To account for realistic operative conditions, $p_0 = 0.4$ mbar and $\nu = 3.1 \times 10^8$ Hz have been assumed [35]. Notably, $|\Gamma| > -1$ dB regardless

TABLE 1. Comparison between plasma-based elements and other unit cells adopted in IRSs.

Technology	Min. $\|\Gamma\|$ [dB]	Thickness [mm]	f [GHz]
Plasma	-1	$10-30$	10
PIN diode [36]	-5	7	$9.4-11.4$
PIN diode [37]	-6	3	$32.5-40.5$
Varactor diode [38]	-7	6	$11.0-12.0$
Varactor diode [39]	-4	5	$5.3-5.5$
MEMS switchers [40]	-6	3	$9.4-11.4$

of the values of n_e and z_{pl}; the minimum value is registered for $n_e \approx n_e^{cr}$, its magnitude decreases with z_{pl}. The span in which the phase of Γ can be controlled varying n_e (i.e., electronically) depends on z_{pl}; a reconfigurability over 360 deg is physically achievable for $z_{pl} > \lambda/2$.

Result in terms of $|\Gamma|$ can be interpreted considering that $\mathrm{Im}(\varepsilon_r)$ increases with ω_p (see Eq. 1), namely, Ohmic losses grow with n_e [29]. Nonetheless, in the dielectric regime ($\mathrm{Re}(\varepsilon_r) > 0$) EM waves propagate within the plasma, while in the conductor regime ($\mathrm{Re}(\varepsilon_r) < 0$) the incident wave is almost completely reflected at the air-plasma interface. In other words, a significant mismatching between Z_{pl} and the impedance of the free space occurs for $n_e \gtrsim n_e^{cr}$: Z_{pl} tends to the infinity for $n_e = n_e^{cr}$ and it is mostly imaginary in the conductor regime. As a result, the condition $n_e \approx n_e^{cr}$ is critical since the incident wave, before being reflected, propagates in a medium where non-negligible Ohmic losses occur. Moreover, the thicker the plasma slab, the higher the total power dissipated within the lossy medium (see Eq. 11).

For what the phase of Γ is concerned, it tends to -180 deg for $n_e > 10^{19}$ m^{-3} since the plasma behaves as a good conductor (i.e., poor matching between Z_{pl} and Z_0). On the other hand, when $n_e \longrightarrow 0$ (i.e., $Z_{pl} \approx Z_0$), the value of $\mathrm{ang}(\Gamma)$ depends only on the distance z_{pl} between the ground plane, where the incident wave is reflected, and the edge of the plasma cell. As a result, $z_{pl} = \lambda/2$ is the threshold distance to control the phase over 360 deg provided that for $n_e = 0$ the incident wave is reflected in the ground plane, while for $n_e \gg 10^{19}$ m^{-3} it is reflected in the edge of the plasma cell. The larger z_{pl},the smaller the maximum value of n_e required to reconfigure the phase over 360 deg. Namely, $z_{pl} = \lambda/2$ is a physical threshold to control the phase over 360 deg. However, considering the plasma production technology at the state-of-the-art [4], the condition $z_{pl} \approx \lambda$ is a more realistic lower bound.

From a technological standpoint, realizing a plasma-based IRS is feasible since plasma allows full control of the phase of the reflected wave while ensuring $|\Gamma|$ close to the unit. The latter is a remarkable advantage over classical solutions [33] where $|\Gamma|$ usually drops in correspondence of $\mathrm{ang}(\Gamma) = 0$ [34]. In unit cells based on PIN diodes, varactor diodes, or MEMS switchers, $|\Gamma|$ can be up to 6 dB lower with respect to plasma-based systems (see Table 1). On the other hand, plasma elements shall be relatively thicker than classical unit cells to guarantee a sufficient control of the phase: in the order of λ instead of 0.10–0.30 λ. Nevertheless, suppose the intended application can be accomplished by relying on digital elements [41], [42], namely controlling the phase only in a discrete range of values (say 180 deg). In that case, the constraint on the plasma thickness can be relaxed (see Section IV).

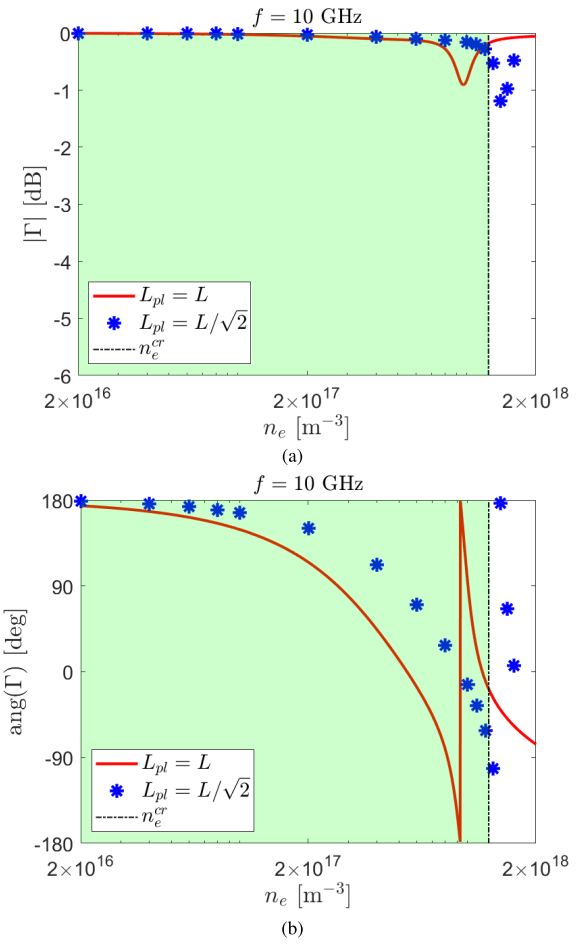

FIGURE 5. (a) Magnitude, and (b) phase of the reflection coefficient Γ in function of the plasma density n_e. Comparison between different values of the plasma width L_{pl}. $L = \lambda/2$, $z_{pl} = \lambda$, $n_0 = 10^{22}$ m^{-3} ($p_0 = 0.4$ mbar), and $\nu = 3.1 \times 10^8$ Hz. Green background indicates the dielectric regime, white background the conductor regime.

IV. NUMERICAL ANALYSIS

The numerical model described in Section II has been exploited to define the preliminary design of plasma-based IRSs. First, the behaviour of a plasma element has been assessed by accounting for practical constraints (e.g., $L_{pl} \neq L$). Second, the design of two IRSs is proposed. The former exploits thick plasma elements ($z_{pl} = \lambda$) to accomplish beam steering operations via a continuous control of the phase. The latter relies on digital plasma elements whose thickness is $z_{pl} = \lambda/3$ to produce specific diffraction patterns.

A. PLASMA ELEMENT DESIGN

The condition $L_{pl} = L$ is hardly met in practice since additional equipment is required to confine and ignite the plasma

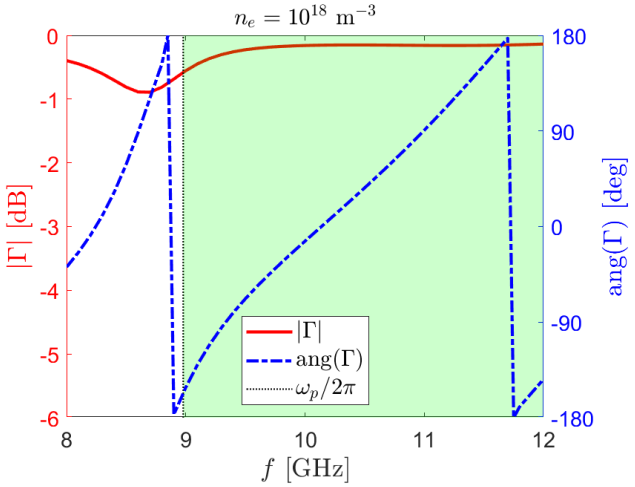

FIGURE 6. Magnitude, and phase of the reflection coefficient Γ in function of the operation frequency f for $n_e = 10^{18}$ m^{-3}. $z_{pl} = 30$ mm, $L = 15$ mm, $L_{pl} = L/\sqrt{2}$, $n_0 = 10^{22}$ m^{-3} ($p_0 = 0.4$ mbar), and $\nu = 3.1 \times 10^8$ Hz. Green background indicates the dielectric regime, white background the conductor regime.

TABLE 2. Properties of the plasma elements that constitute the IRS depicted in Fig. 7. $z_{pl} = \lambda$, $n_0 = 10^{22}$ m^{-3} ($p_0 = 0.4$ mbar), and $\nu = 3.1 \times 10^8$ Hz.

Column	n_e [m^{-3}]	ω_p [rad/s]	$\lvert\Gamma\rvert$ [dB]	ang(Γ) [deg]
1	0	0	0	180
2	2.1×10^{17}	2.6×10^{10}	-0.03	149
3	3.8×10^{17}	3.4×10^{10}	-0.06	117
4	5.3×10^{17}	4.1×10^{10}	-0.08	86
5	6.7×10^{17}	4.6×10^{10}	-0.11	55
6	8.2×10^{17}	5.1×10^{10}	-0.13	24
7	9.7×10^{17}	5.5×10^{10}	-0.15	-8
8	1.1×10^{18}	5.9×10^{10}	-0.20	-39
9	1.2×10^{18}	6.3×10^{10}	-0.31	-70
10	1.3×10^{18}	6.4×10^{10}	-0.53	-102

(e.g., vessels that contain neutral gas and electrodes) [43]. Therefore, the theoretical configuration $L_{pl} = L$ has been compared against a plasma element where $L_{pl} = L/\sqrt{2}$ (see Fig. 5) [16]. The operation frequency is $f = 10$ GHz [34], namely $L = \lambda/2 = 15$ mm and $z_{pl} = \lambda = 30$ mm. The former condition guarantees a periodicity of the plasma elements that avoids grating lobes [44]. The latter assumption on z_{pl} is intended to guarantee a 360 deg control of the phase relying on affordable plasma density values. Plasma parameters are selected according to the usual operative conditions of GPAs [35]: $p_0 = 0.4$ mbar and $\nu = 3.1 \times 10^8$ Hz. Regardless of the value of L_{pl}/L, similar trends are obtained in terms of both the magnitude and phase of Γ. The most relevant difference is that the value of n_e required to control the phase over 360 deg is higher for $L_p = L/\sqrt{2}$: $n_e = 1.4 \times 10^{18}$ m^{-3} instead of $n_e = 0.9 \times 10^{18}$ m^{-3}. This is not a major issue since such a value of n_e is compatible with the plasma production technology at the state-of-the-art [35].

The configuration $L_{pl} = L/\sqrt{2}$ has been further analysed in Fig. 6 to evaluate the response of the plasma element in a frequency range from 8 GHz up to 12 GHz, namely ±2 GHz with respect to the central frequency $f = 10$ GHz. The condition $|\Gamma| > -1$ dB is maintained within the range of interest. At the central frequency ang(Γ) = −13 deg, the phase of Γ spans from -90 deg up to 90 deg in an interval larger than 1 GHz. Namely, these plasma elements present a bandwidth several times larger than many classical systems where it spans 0.1–0.2 GHz [34], [45].

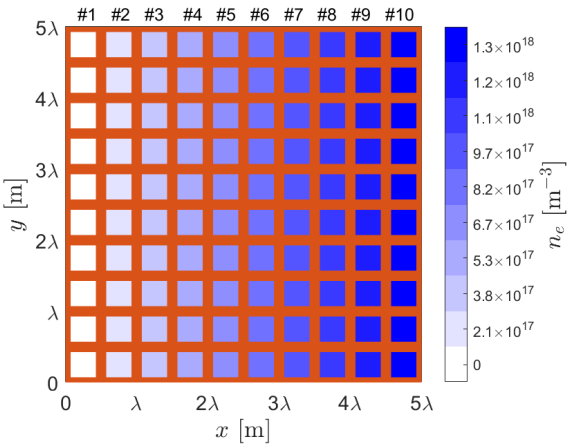

FIGURE 7. Schematic of the plasma-based IRS. Each plasma element is colored according to the color scale, and indicates the corresponding plasma density n_e. Numbering (#) refers to the columns of the array.

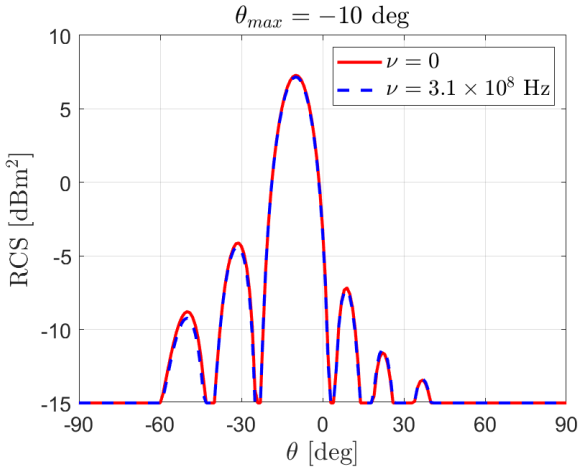

FIGURE 8. Radar Cross Section vs azimuth angle θ (x–z plane) of the plasma-based IRS depicted in Fig. 7, for collisionless ($\nu = 0$, solid red curve) and collisional ($\nu = 3.1 \times 10^8$ Hz, dashed blue curve) plasma.

B. IRS - CONTINUOUS PHASE SHIFT

The plasma element described in Section IV-A, has been exploited to design an IRS in which n_e and, in turn, the phase of Γ can be controlled continuously to enable beam steering operations. An IRS made of 10 × 10 plasma elements constitutes the design (see Fig. 7) [16]. The operation frequency is $f = 10$ GHz, and the element periodicity has been chosen as $L = \lambda/2 = 15$ mm to avoid grating lobes [44]. Specifically, n_e has been varied column by column to steer the beam along the direction $\theta_{max} = -10$ deg on the x–z plane

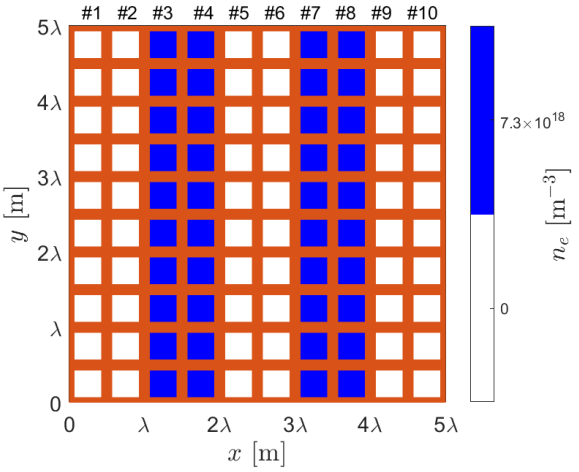

FIGURE 9. Schematic of the IRS based on digital plasma elements. Each plasma element is colored according to the color scale, and indicates the corresponding plasma density n_e. Numbering (#) refers to the columns of the array.

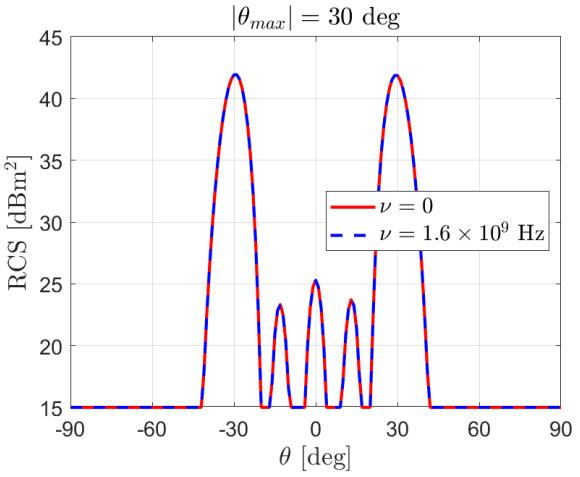

FIGURE 10. Radar Cross Section vs azimuth angle θ (x–z plane) for the plasma-based IRS depicted in Fig. 9, for collisionless ($\nu = 0$, solid red curve) and collisional ($\nu = 1.6 \times 10^9$ Hz, dashed blue curve) plasma.

TABLE 3. Properties of the digital plasma elements that constitute the IRS depicted in Fig. 9. $z_{pl} = \lambda/3$, $n_0 = 5 \times 10^{22}$ m^{-3} ($p_0 = 2.0$ mbar), and $\nu = 1.6 \times 10^9$ Hz.

Column	n_e [m^{-3}]	ω_p [rad/s]	$\lvert\Gamma\rvert$ [dB]	ang(Γ) [deg]
1, 2, 5, 6, 9, 10	0	0	0	57
3, 4, 7, 8	7.3×10^{18}	1.5×10^{11}	-0.27	-133

(broadside in correspondence of $\theta = 0$). The properties of the plasma elements, sorted by column, are reported in Table 2. In addition, the array factor rule has been adopted to design the plasma panel, with n_e tuned to impose a constant phase shift β between the elements of each column. Precisely, the phase shift β reads [44]

$$\beta = \frac{2\pi L}{\lambda} \sin\theta_{max} = -31 \text{ deg}. \tag{12}$$

This methodology allows for designing of an IRS that perfectly matches the requirement in terms of θ_{max} (see Fig 8). It is worth noting that the RCS has been computed for both a collisional and a collisionless plasma. Specifically, power losses are neglected in the collisionless case since $\nu = 0$ and therefore $|\Gamma| = 0$ dB. Vice versa, they are accounted for a collisional plasma where $\nu = 3.1 \times 10^8$ Hz and, in turn, $|\Gamma| \neq 0$ dB (see Table 2). Very comparable results are obtained for the two cases (differences < 0.1 dBm^2), confirming that negligible power losses occur within a plasma cell that exploits realistic plasma properties [35].

C. IRS - DIGITAL ELEMENTS

A plasma-based IRS has been designed relying on digital elements, and, to prove the feasibility of this concept, a 1-Bit coding implementation is investigated. Two states characterize each plasma element, "on" and "off," respectively, that present a phase difference of about 180 deg [42], [46], [47]. The parameters of this IRS follow: operation frequency $f = 10$ GHz, lattice periodicity, $L = \lambda/2 = 15$ mm, plasma element width, $L_{pl} = L/\sqrt{2}$, and thickness, $z_{pl} = \lambda/3 = 10$ mm. This design employs a relatively thin plasma cell since there is no need to control the phase over 360 deg. Indeed, the value $z_{pl} = \lambda/3$ is a trade-off between compactness and achievable plasma properties. Provided that a plasma density in the order of $n_e \approx 10^{19}$ m^{-3} is required for this application (see Fig. 4), the neutral pressure is assumed to be $p_0 = 2$ mbar, and $\nu = 1.6 \times 10^9$ Hz [5], [9]. In fact, according to experimental evidence [4] and theoretical prediction [6], in usual GPAs higher values of n_e are achievable increasing p_0. Again, a structure of 10×10 plasma elements constitutes the proposed IRS (see Fig. 9). The "on"–"off" state of each column has been controlled to achieve $|\theta_{max}| = 30$ deg; the assumed plasma properties are reported in Table 3. The fulfillment of the requirement imposed on θ_{max} is demonstrated in Fig. 10 where the obtained RCS is depicted. Specifically, $n_e = 7.3 \times 10^{18}$ m^{-3} is required for the "on" state, which is a value fully compatible with the technology at the state-of-the-art [5], [9]. Provided that neutral pressure is higher with respect to the cases analysed in previous sections (i.e., higher losses might occur within plasma [6]), the RCS computed assuming $\nu = 0$ has been depicted in Fig. 10. The results are very comparable with the collisional case (differences < 0.2 dBm^2) consistently with a value of $|\Gamma|$ close to the unit for the plasma elements adopted in this design (see Table 3).

It is worth noting that plasma-based IRSs relying on multi-Bits elements are feasible but have not been analysed in this work for the sake of brevity. Specifically, multi-Bits designs present a better power efficiency with respect to 1-Bit implementations [48] but require thicker plasma cells. For example, $z_{pl} = \lambda/2$ may be sufficient to guarantee a 2-Bit phase resolution where the four states need to encompass a phase increment of 90 deg. The latter concept is particularly appealing for high gain IRS targeted at massive multiple-input multiple-output applications [45].

V. CONCLUSION AND FUTURE WORK

A feasibility study has been accomplished to assess the use of plasma to realize IRSs. To this end, a theoretical model has been developed to analyse the single plasma element, and numerical simulations have been performed to design the plasma panel. The main advantage of a plasma-based IRS, with respect to classical devices [34], is the possibility to control the phase of the reflected wave while maintaining the magnitude of the reflection coefficient close to the unit. Namely, the Ohmic losses are negligible, even assuming plasma properties achievable with the technology at the state-of-the-art [9]. The need for thick plasma elements (comparable to the wavelength in air, λ) to control the phase of the reflected wave over 360 deg represents the main drawback of such technology. Nonetheless, this constraint can be relaxed if one is interested in a smaller tunability range, such as for digital IRSs. In this work, for example, a 1-Bit digital IRS with a thickness of $\lambda/3$ has been demonstrated. All these features show that plasma-based IRSs are a feasible and appealing technology worth further investigation.

Although the assumed plasma properties are compatible with the state-of-the-art technology [4], a few challenges must be faced to prove the proposed technology's concept. First, the electronics for plasma production shall be optimized and miniaturized since the hardware employed to generate the plasma in GPAs is usually bulky [4], [9]. A similar problem has been solved in the frame of space propulsion, where the electronics for plasma production are miniaturized to be compatible with the CubeSat standards [49], [50]. Second, proper electrodes shall be designed to trigger the plasma production minimizing their EM interference with the propagating waves. Third, an ''intelligent'' control system shall be implemented to trigger the plasma discharge. Remarkably, the last two tasks have been partially solved in the field of plasma display panels for the miniaturization of the plasma production system and the control of multiple elements [43]. Therefore, the consolidated know-how in the fields of plasma antennas, space propulsion, and plasma display panels shall be exploited to realize a proof of concept of a plasma-based IRS. The required level of interdisciplinarity is comparable with other applications involving plasma technology (e.g., plasma medicine) [51], thus plasma-based IRSs can be considered feasible.

Finally, it is worth mentioning that the miniaturization of both the plasma elements and the related electronics is a topical subject nowadays, provided the large interest in millimeter waves [34] and 5G–6G communications [18].

REFERENCES

[1] T. Anderson, *Plasma Antennas*. Norwood, MA, USA: Artech House, 2020.
[2] J. P. Rayner, A. P. Whichello, and A. D. Cheetham, ''Physical characteristics of plasma antennas,'' *IEEE Trans. Plasma Sci.*, vol. 32, no. 1, pp. 269–281, Feb. 2004.
[3] T. Naito, S. Yamaura, Y. Fukuma, and O. Sakai, ''Radiation characteristics of input power from surface wave sustained plasma antenna,'' *Phys. Plasmas*, vol. 23, no. 9, 2016, Art. no. 093504.
[4] A. Daykin-Iliopoulos, F. Bosi, F. Coccaro, M. Magarotto, A. Papadimopoulos, P. D. Carlo, C. Dobranszki, I. Golosnoy, and S. Gabriel, ''Characterisation of a thermionic plasma source apparatus for high-density gaseous plasma antenna applications,'' *Plasma Sources Sci. Technol.*, vol. 29, no. 11, 2020, Art. no. 115002.
[5] P. D. Carlo, M. Magarotto, G. Mansutti, A. Selmo, A.-D. Capobianco, and D. Pavarin, ''Feasibility study of a novel class of plasma antennas for SatCom navigation systems,'' *Acta Astronautica*, vol. 178, pp. 846–853, Jan. 2021.
[6] M. Magarotto, P. de Carlo, G. Mansutti, F. J. Bosi, N. E. Buris, A.-D. Capobianco, and D. Pavarin, ''Numerical suite for gaseous plasma antennas simulation,'' *IEEE Trans. Plasma Sci.*, vol. 49, no. 1, pp. 285–297, Jan. 2021.
[7] J. Zhao, L. Kong, X. Chen, H. Liu, and S. Wang, ''Experimental study on a self-phase-shifting cross vibrator plasma antenna array,'' *IEEE Antennas Wireless Propag. Lett.*, vol. 21, no. 7, pp. 1343–1347, Jul. 2022.
[8] G. G. Borg, J. H. Harris, N. M. Martin, D. Thorncraft, R. Milliken, D. G. Miljak, B. Kwan, T. Ng, and J. Kircher, ''Plasmas as antennas: Theory, experiment and applications,'' *Phys. Plasmas*, vol. 7, no. 5, pp. 2198–2202, May 2000.
[9] P. De Carlo, M. Magarotto, G. Mansutti, S. Boscolo, A.-D. Capobianco, and D. Pavarin, ''Experimental characterization of a plasma dipole in the UHF band,'' *IEEE Antennas Wireless Propag. Lett.*, vol. 20, no. 9, pp. 1621–1625, Sep. 2021.
[10] G. Mansutti, P. D. Carlo, M. A. Hannan, F. Boulos, P. Rocca, A.-D. Capobianco, M. Magarotto, and A. Tuozzi, ''Modeling and design of a plasma-based transmit-array with beam scanning capabilities,'' *Results Phys.*, vol. 16, Mar. 2020, Art. no. 102923.
[11] G. Mansutti, P. D. Carlo, M. Magarotto, M. A. Hannan, P. Rocca, A.-D. Capobianco, D. Pavarin, and A. Tuozzi, ''Design of a hybrid metal-plasma transmit-array with beam-scanning capabilities,'' *IEEE Trans. Plasma Sci.*, vol. 50, no. 3, pp. 662–669, Mar. 2022.
[12] G. Mansutti, D. Melazzi, and A.-D. Capobianco, ''A reconfigurable metal-plasma Yagi–Yuda antenna for microwave applications,'' *Adv. Sci. Technol. Eng. Syst. J.*, vol. 2, no. 3, pp. 441–448, 2017.
[13] H. A. Malhat, M. M. Badawy, S. H. Zainud-Deen, and K. H. Awadalla, ''Dual-mode plasma reflectarray/transmitarray antennas,'' *IEEE Trans. Plasma Sci.*, vol. 43, no. 10, pp. 3582–3589, Oct. 2015.
[14] D. Melazzi, P. D. Carlo, F. Trezzolani, M. Manente, A. D. Capobianco, and S. Boscolo, ''Beam-forming capabilities of a plasma circular reflector antenna,'' *IET Microw. Antenna Propag.*, vol. 12, no. 15, pp. 2301–2306, Jul. 2018.
[15] M. T. Jusoh, O. Lafond, F. Colombel, and M. Himdi, ''Performance and radiation patterns of a reconfigurable plasma corner-reflector antenna,'' *IEEE Antennas Wireless Propag. Lett.*, vol. 12, pp. 1137–1140, 2013.
[16] S. H. Zainud-Deen, H. A. Malhat, S. M. Gaber, M. Ibrahim, and K. H. Awadalla, ''Plasma reflectarrays,'' *Plasmonics*, vol. 8, no. 3, pp. 1469–1475, Sep. 2013.
[17] W. Saad, M. Bennis, and M. Chen, ''A vision of 6G wireless systems: Applications, trends, technologies, and open research problems,'' *IEEE Netw.*, vol. 34, no. 3, pp. 134–142, May/Jun. 2020.
[18] *Metawave Announce Successful Demonstration of 28 GHz-Band 5G Using World's First Meta-Structure Technology*, NTT DoCoMo, Tokyo, Japan, 2018.
[19] E. Basar, M. D. Renzo, J. D. Rosny, M. Debbah, M. Alouini, and R. Zhang, ''Wireless communications through reconfigurable intelligent surfaces,'' *IEEE Access*, vol. 7, pp. 116753–116773, 2019.
[20] S. Hu, F. Rusek, and O. Edfors, ''Beyond massive MIMO: The potential of positioning with large intelligent surfaces,'' *IEEE Trans. Signal Process.*, vol. 66, no. 7, pp. 1761–1774, Apr. 2018.
[21] Y. Liu, X. Liu, X. Mu, T. Hou, J. Xu, M. Di Renzo, and N. Al-Dhahir, ''Reconfigurable intelligent surfaces: Principles and opportunities,'' *IEEE Commun. Surveys Tuts.*, vol. 23, no. 3, pp. 1546–1577, 3rd Quart., 2021.
[22] V. Tapio, I. Hemadeh, A. Mourad, A. Shojaeifard, and M. Juntti, ''Survey on reconfigurable intelligent surfaces below 10 GHz,'' *EURASIP J. Wireless Commun. Netw.*, vol. 2021, no. 1, pp. 1–18, 2021.
[23] Y. Yuan, S. Sun, Y. Chen, K. Zhang, X. Ding, B. Ratni, Q. Wu, S. N. Burokur, and C.-W. Qiu, ''A fully phase-modulated metasurface as an energy-controllable circular polarization router,'' *Adv. Sci.*, vol. 7, no. 18, 2020, Art. no. 2001437.
[24] K. Zhang, Y. Wang, S. N. Burokur, and Q. Wu, ''Generating dual-polarized vortex beam by detour phase: From phase gradient metasurfaces to metagratings,'' *IEEE Trans. Microw. Theory Techn.*, vol. 70, no. 1, pp. 200–209, Jan. 2022.
[25] X. Tan, Z. Sun, J. M. Jornet, and D. Pados, ''Increasing indoor spectrum sharing capacity using smart reflect-array,'' in *Proc. IEEE Int. Conf. Commun. (ICC)*, May 2016, pp. 1–6.
[26] Q. Wu and R. Zhang, ''Towards smart and reconfigurable environment: Intelligent reflecting surface aided wireless network,'' *IEEE Commun. Mag.*, vol. 58, no. 1, pp. 106–112, Nov. 2019.

[27] M. D. Renzo, A. Zappone, M. Debbah, M.-S. Alouini, C. Yuen, J. D. Rosny, and S. Tretyakov, "Smart radio environments empowered by reconfigurable intelligent surfaces: How it works, state of research, and the road ahead," *IEEE J. Sel. Areas Commun.*, vol. 38, no. 11, pp. 2450–2525, Nov. 2020.
[28] D. Melazzi, V. Lancellotti, and A.-D. Capobianco, "Analytical and numerical study of a gaseous plasma dipole in the UHF frequency band," *IEEE Trans. Antennas Propag.*, vol. 65, no. 12, pp. 7091–7101, Dec. 2017.
[29] J. A. Bittencourt, *Fundamentals of Plasma Physics*. Cham, Switzerland: Springer, 2004.
[30] N. Souhair, M. Magarotto, E. Majorana, F. Ponti, and D. Pavarin, "Development of a lumping methodology for the analysis of the excited states in plasma discharges operated with argon, neon, krypton, and xenon," *Phys. Plasmas*, vol. 28, no. 9, 2021, Art. no. 093504.
[31] M. A. Lieberman and A. J. Lichtenberg, *Principles of Plasma Discharges and Materials Processing*. Hoboken, NJ, USA: Wiley, 2005.
[32] F. T. Ulaby, E. Michielssen, and U. Ravaioli, *Fundamentals of Applied Electromagnetics*, vol. 7. Upper Saddle River, NJ, USA: Pearson, 2015.
[33] F. Costa and M. Borgese, "Electromagnetic model of reflective intelligent surfaces," *IEEE Open J. Commun. Soc.*, vol. 2, pp. 1577–1589, 2021.
[34] Q. Wu, S. Zhang, B. Zheng, C. You, and R. Zhang, "Intelligent reflecting surface-aided wireless communications: A tutorial," *IEEE Trans. Commun.*, vol. 69, no. 5, pp. 3313–3351, May 2021.
[35] F. Sadeghikia, M. T. Noghani, and M. R. Simard, "Experimental study on the surface wave driven plasma antenna," *AEU-Int. J. Electron. Commun.*, vol. 70, no. 5, pp. 652–656, May 2016.
[36] E. Carrasco, M. Barba, and J. A. Encinar, "X-band reflectarray antenna with switching-beam using PIN diodes and gathered elements," *IEEE Trans. Antennas Propag.*, vol. 60, no. 12, pp. 5700–5708, Dec. 2012.
[37] J. Rodriguez-Zamudio, J. I. Martinez-Lopez, J. Rodriguez-Cuevas, and A. E. Martynyuk, "Reconfigurable reflectarrays based on optimized spiraphase-type elements," *IEEE Trans. Antennas Propag.*, vol. 60, no. 4, pp. 1821–1830, Apr. 2012.
[38] F. Venneri, S. Costanzo, and G. D. Massa, "Design and validation of a reconfigurable single varactor-tuned reflectarray," *IEEE Trans. Antennas Propag.*, vol. 61, no. 2, pp. 635–645, Feb. 2013.
[39] C. Liu and S. V. Hum, "An electronically tunable single-layer reflectarray antenna element with improved bandwidth," *IEEE Antennas Wireless Propag. Lett.*, vol. 9, pp. 1241–1244, 2010.
[40] E. Carrasco, M. Barba, B. Reig, C. Dieppedale, and J. A. Encinar, "Characterization of a reflectarray gathered element with electronic control using ohmic RF MEMS and patches aperture-coupled to a delay line," *IEEE Trans. Antennas Propag.*, vol. 60, no. 9, pp. 4190–4201, Sep. 2012.
[41] H. Yang, F. Yang, S. Xu, Y. Mao, M. Li, X. Cao, and J. Gao, "A 1-bit 10×10 reconfigurable reflectarray antenna: Design, optimization, and experiment," *IEEE Trans. Antennas Propag.*, vol. 64, no. 6, pp. 2246–2254, Jun. 2016.
[42] T. J. Cui, M. Q. Qi, X. Wan, J. Zhao, and Q. Cheng, "Coding metamaterials, digital metamaterials and programmable metamaterials," *Light, Sci. Appl.*, vol. 3, no. 10, p. e218, 2014.
[43] J. Boeuf, "Plasma display panels: Physics, recent developments and key issues," *J. Phys. D, Appl. Phys.*, vol. 36, no. 6, p. R53, 2003.
[44] C. A. Balanis, *Antenna Theory: Analysis and Design*. Hoboken, NJ, USA: Wiley, 2015.
[45] L. Dai, B. Wang, M. Wang, X. Yang, J. Tan, S. Bi, S. Xu, F. Yang, Z. Chen, M. D. Renzo, C.-B. Chae, and L. Hanzo, "Reconfigurable intelligent surface-based wireless communications: Antenna design, prototyping, and experimental results," *IEEE Access*, vol. 8, pp. 45913–45923, 2020.
[46] H. Kamoda, T. Iwasaki, J. Tsumochi, T. Kuki, and O. Hashimoto, "60-GHz electronically reconfigurable large reflectarray using single-bit phase shifters," *IEEE Trans. Antennas Propag.*, vol. 59, no. 7, pp. 2524–2531, Jul. 2011.
[47] X. Tan, Z. Sun, D. Koutsonikolas, and J. M. Jornet, "Enabling indoor mobile millimeter-wave networks based on smart reflect-arrays," in *Proc. IEEE INFOCOM Conf. Comput. Commun.*, Apr. 2018, pp. 270–278.
[48] Q. Wu and R. Zhang, "Beamforming optimization for intelligent reflecting surface with discrete phase shifts," in *Proc. IEEE Int. Conf. Acoust., Speech Signal Process. (ICASSP)*, May 2019, pp. 7830–7833.
[49] N. Bellomo, "Design and in-orbit demonstration of regulus, an iodine electric propulsion system," *CEAS Space J.*, vol. 14, no. 1, pp. 79–90, 2022.
[50] M. Manente, F. Trezzolani, M. Magarotto, E. Fantino, A. Selmo, N. Bellomo, E. Toson, and D. Pavarin, "REGULUS: A propulsion platform to boost small satellite missions," *Acta Astronautica*, vol. 157, pp. 241–249, Apr. 2019.
[51] I. Adamovich, S. Baalrud, A. Bogaerts, P. Bruggeman, M. Cappelli, V. Colombo, U. Czarnetzki, U. Ebert, J. Eden, and P. Favia, "The 2017 plasma roadmap: Low temperature plasma science and technology," *J. Phys. D, Appl. Phys.*, vol. 50, no. 32, 2017, Art. no. 323001.
l

MIRKO MAGAROTTO received the M.Eng. degree in aerospace engineering and the Ph.D. degree in science technology and measurements for space from the University of Padova, Padova, Italy, in 2015 and 2019, respectively. He is currently a Research Fellow with the University of Padova, where he is a member of the Space Propulsion Group. His current research interests include plasma numerical simulation, plasma antennas, and electric plasma propulsion.

LUCA SCHENATO (Member, IEEE) received the B.Sc. degree in telecommunication engineering and the Ph.D. degree in electronic and telecommunication engineering from the University of Padova, Padova, Italy, in 2003 and 2007, respectively. He is currently a Researcher at the Italian National Research Council in Padova. His current research interests include optical fiber sensors, optical fiber-based devices, and intelligent reflective surfaces.

PAOLA DE CARLO received the M.Eng. degree in aerospace engineering and the Ph.D. degree in science technology and measurements for space from the University of Padova, in 2014 and 2018, respectively. She was a postdoctoral fellow for four years. She is currently a Project Engineer with Technology for Propulsion and Innovation S.P.A, where she works on plasma space propulsion. Her main research interests include plasma antenna and plasma sources for telecommunications.

ANTONIO-DANIELE CAPOBIANCO (Member, IEEE) received the B.Sc. degree in electronic engineering and the Ph.D. degree in electronic and telecommunication engineering from the University of Padova, Padova, Italy, in 1989 and 1994, respectively. He is currently an Associate Professor with the Department of Information Engineering, University of Padova. His current research interests include theory and numerical modeling in the fields of photonics, plasmonics, and microwave antennas.